TOWARDS DESIGN RULES FOR RECTANGULAR SILO FILLING PRESSURES

J.M. Rotter†, R.J. Goodey*and C.J. Brown‡[a]

† University of Edinburgh, Institute for Infrastructure and Environment, The King's Buildings, Edinburgh EH9 3JN, UK.

* City, University of London, School of Mathematics, Computer Science & Engineering, London EC1V 0HB, UK.

‡[a] Brunel University London, College of Engineering Design and Physical Sciences, Uxbridge UB8 3PH, UK.

[a] Author to receive correspondence.

Abstract: *An experimentally validated finite element model of filling pressures in rectangular silos with flexible walls is used to predict the stress regime in the stored solid in squat and intermediate aspect ratio silos. The model predicts the state of stress in the stored solid and the pressures imposed on the flexible walls of the silo. The non-uniform horizontal pressure distributions at each depth at the end of filling are explored. It is known that an empirical relation for the horizontal pressure variation on each straight wall derived from experimental observations in an earlier study closely matches the computational predictions. The coefficients of this relation are found to vary with depth below the stored solid surface, and depend on the relative stiffness of stored solid and the silo wall. Following many calculations involving different solids, an empirical relationship is derived that is suitable for practical design for a range of different stored solids for which relevant properties are known. The resulting expression is well suited to the practical determination of filling pressures in rectangular silos, and provides a silo design pressure proposal that is based on theoretical, rather than empirical findings.*

Keywords

Pressures, silos, square silos, rectangular silos, design rules, filling, flexible wall, horizontal distribution.

1.0 Introduction

Silos are sometimes required in locations where space is very limited. Under these conditions, a rectangular cross-section or planform provides a good economic solution, and multiple silos can be tessellated. However, the structure of a rectangular planform silo must be designed to sustain both bending and stretching (membrane) actions [1-3], whilst those of a circular silo are predominantly designed for membrane forces [1, 3-7]. Where a rectangular silo is constructed in steel, the walls may be made relatively thin if the pattern of pressures on the wall is well understood, and a thin wall itself reduces the pressures at the mid-side of the wall [8]. The required wall thickness for a rectangular silo is very sensitive to the bending moments that develop in the walls, and these in turn depend very much on the distribution and magnitude of the pressures on the wall. This paper explores the pressure patterns in silos containing different solids and produces design recommendations for both the pattern and magnitudes of pressures on moderately flexible walls in rectangular planform silos. These non-uniform pressure patterns might be used directly to produce extremely efficient structural designs.

Wall pressure predictions in standards are almost universally based on the equilibrium of a horizontal slice of stored granular solid [9,10] often using the assumption of a constant value for the lateral pressure ratio K_m (the ratio of mean horizontal wall pressure to mean vertical stress in the granular solid at any level). Janssen's original paper suggested that the mid-side of each wall in a rectangular silo might experience an increase in normal pressure, and this idea was reinforced by a few sample finite element predictions [11] in which the walls were treated as rigid. By contrast, experimental observations [8,12,13] in steel silos have shown that there is a substantial pressure reduction at the mid-side of each wall. Many authors [e.g.14-19] used the finite element method to assess the pressures in circular silos during both filling and discharge. A significant review of the earlier work was made by Rotter *et al* [20]. However, none of these studies led to design rules that relate the

calculated pressures to the properties of the stored solid. Moreover, relatively few calculations have been made for rectangular silos, and none appear to have included the wall as a flexible element when considering structural design.

This paper exploits a large body of predictions of filling pressures produced by a finite element model that was validated against detailed careful experiments on thin-walled square steel silos, in which significant wall flexural deformations developed by the end of the filling process. The predicted pressure patterns on the silo walls were found to closely match the simple empirical relationship previously developed by the authors from experimental measurements [21]. Following an extensive parametric study, practical design rules are developed for filling pressures in rectangular planform silos, relating the pattern and magnitudes of the wall pressures to the properties of the stored solid.

2.0 Materials and Methods

2.1 Finite element modelling and the constitutive law

The finite element method has been exploited to predict pressures in silos by treating the granular solid as a continuum by many authors [14-18, 22-27]. In this study, the commercial code ABAQUS [28] was used to develop a reliable model for the filling pressures in square and rectangular silos with flexible walls, and was validated against detailed experiments [29-31]. A close match with the measured filling pressures in the granular bulk solid was achieved using the porous elastic model with Drucker-Prager plasticity (PE-DP) constitutive law to describe the stored solid. This law was also previously successfully applied to silo problems [26,32,34]. The porous elastic model is based on the isotropic compression response of critical state soil mechanics [e.g. 35] in which the stiffness of the solid is dependent on the stress level and stress history. The parameters that must be used in this model are discussed below. A key advantage in using the validated finite element model is the capability to represent different stored materials through change in a limited set of material parameters.

The details of the validated model has been presented extensively elsewhere [30-31]. One quarter of the structure was modelled, and the corner where the box and hopper walls meet was restrained against vertical movement. Symmetry conditions were applied to the cut vertical boundaries. The structural model used 4-noded quadrilateral shell elements of isotropic elastic mild steel with E =

210GPa and ν = 0.3. The stored granular solid was modelled using 8-noded brick continuum elements. Two natural granular solids (Leighton Buzzard sand and Pea Gravel) were used in the validation, but this paper covers a wider range of solids, with a range of properties. This treatment was used to ensure easy generalisation of the results to all free-flowing solids.

The value of K_m was taken from the Eurocode [36] on silo loads:

$$K_m = 1.1\,(1 - \sin\,\phi_i) \tag{1}$$

where ϕ_i is the loading angle of internal friction. Poisson's ratio ν was obtained from this expression assuming that it derives from compression of an isotropic elastic solid in a smooth-walled rigid container [37] as:

$$\nu = \frac{K_m}{1 + K_m} \qquad \text{or} \qquad K_m = \frac{\nu}{1 - \nu} \tag{2}$$

leading to:

$$\nu = \frac{(1 - \sin\,\phi_i)}{(1.91 - \sin\,\phi_i)} \tag{3}$$

This value of Poisson's ratio was used only during the initial elastic phase of the filling of the silo and consequently has a weak impact on the pressure patterns that were calculated. A range of values for Poisson's ratio is given in the Appendix using values of ϕ_i from EN1991-4.

The most important parameter in describing a porous elastic granular solid is the compressibility coefficient λ, as described by Muir Wood, which is the slope of the plot of specific volume against the natural log of the isotropic stress p_I. This coefficient and the initial voids ratio e_0 at a defined pressure p_o are used by the numerical model to define the elastic volumetric behaviour. The compressibility coefficient λ is a measure of the flexibility of the solid; a lower value of the compressibility coefficient λ represents a stiffer solid.

Values for the compressibility coefficient λ in the pressure range appropriate for silos (< 100kPa) have rarely been published. It should also be noted that the initial conditions for filling in a silo (and hence for an initial mean pressure p_o and corresponding voids ratio e_o) are not easy to define because of the sensitivity to filling method. Tests for material properties that use "hand" filling tend to produce

higher initial voids than those adopting a rain fill technique [e.g. 38] where high but repeatable densities are achieved. The best work on this was probably that of Ooi [39]. Evaluation of an appropriate value for λ for a given solid may be subject to some variation. Been *et al* [40] determined the value 0.02 for quartzitic sand, but the Leighton Buzzard sand used in the tests used to validate this analysis [8] has a much higher density and stiffness, so a much lower value than 0.02 should be used for the compressibility coefficient. Goodey *et al* [29] described a simple uniaxial compression test from which the approximate values of 0.002 for Leighton Buzzard sand and 0.0025 for pea gravel were deduced. Values for wheat are taken from Ooi [39].

In the plasticity model, non-dilational flow was assumed with a very small nominal value of cohesion to ensure numerical stability. For the interface between the solid and the wall, a Coulomb friction model was adopted with a constant friction coefficient μ. Table 1 gives the properties used.

Parameter	Leighton Buzzard Sand	Pea Gravel	Wheat
Compressibility coefficient, λ	0.002	0.0025	0.015
Poisson's ratio, ν	0.316	0.306	0.369
Initial voids ratio, e	0.64	0.56	0.80
Cohesion, c	0.1 kPa	0.1 kPa	0.1 kPa
Internal angle of friction, ϕ	45.1°	46.1°	39.1°
Initial Bulk density	1587 kg/m^3	1704 kg/m^3	761 kg/m^3
Coefficient of wall friction, μ	0.445	0.392	0.440

Table 1 – Properties used in finite element model

The filling process was modelled by increasing gravity incrementally until the full value of the granular solid self-weight was reached. This calculation procedure leads to little difference from a progressive layered filling calculation in square silos [41].

3.0 Results

3.1 Verification of FE model predictions by comparison with test observations

Goodey *et al* [29] presented extensive results to show that an FE model using the parameters described above gives excellent predictions of the experimental observations determined from a series of tests on the filling of pilot-scale square silos. A comparison between the mean wall pressures predicted by finite element (FE) analysis (found by integrating horizontally across the wall at the given height) and the Janssen value for one of the experimental silos shows excellent agreement for both of the stored materials used [8,42].

Furthermore, the variation of pressure at any level [21,31] is also well predicted by the FE model, and the general distribution of stress within the stored solid shows good agreement. It is therefore reasonable to conclude that this FE model produces an adequate representation of the phenomena observed in experiments using different structures and different bulk solids, and that this model is adequate as a tool for the more general prediction of rectangular silo filling pressures.

3.1.1 Horizontal pattern of pressure on a flexible wall

The mean value of wall pressure at any level in the experiments is quite accurately predicted by the FE model [29]. Rotter *et al* [21] proposed a model for the horizontal pressure distribution on each wall of a rectangular silo, defined by the two-parameter hyperbolic function

$$p = p_m \left(\frac{\alpha}{\sinh \alpha} \right) \cosh \left(\frac{2\alpha x}{L} \right) \qquad (4)$$

in which p_m is the mean wall pressure at any level, x is the horizontal distance along the wall from the centreline, L is the side-length of the silo and α is a coefficient. The mean wall pressure p_m may be determined as the Janssen value. The coefficient α is important and has been termed the "horizontal non-uniformity coefficient". Further detail of this work has been presented elsewhere [31]. The two-parameter fit (p_m and α) is best characterised in terms of a mid-side and a corner value, with the ratio of corner to mid-side pressure given by cosh α and the ratio of corner to mean value given by α coth α. Uniform pressure across the wall is given by $\alpha = 0$, while increasing positive values of

α indicate increasing ratios of corner to mid-side pressure (a value of α of 2 gives a ratio of corner to mid-side pressures of 3.75).

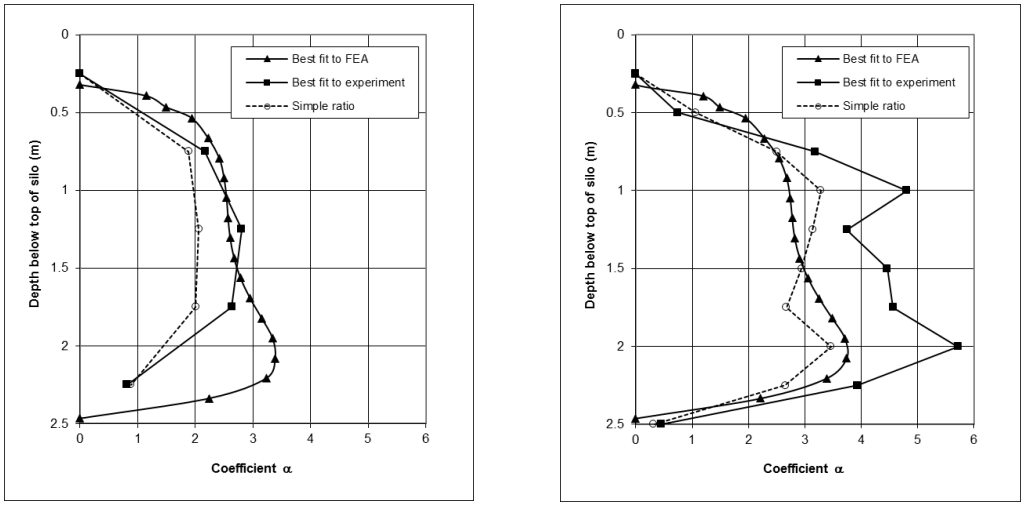

a) b)

Figure 1 - Wall pressure predicted from FE model and two-parameter hyperbolic fit down the wall. a) sand b) gravel

A comparison of the least squares best fit for α to the FE predictions using Eq. 4 is shown in Figure 1 for the 2.5m vertical wall section, where it can be seen that this simple model represents the FE results quite well. The variation down the wall of the least squares best fit value of α for sand from the FE predictions rises from zero at the surface to a stable value of about $\alpha = 2.5$ for the majority of the wall (Figure 1a). Some distance above the transition, the value rises again, achieving a peak of about $\alpha =$ 3.3 before falling back again to zero at the transition. The value previously deduced by Rotter *et al* [21] for the central part of the wall in the experiment was $\alpha = 2.5$ for sand, and this is clearly very close to the value found in the FE calculations.

The best-fit value of the horizontal non-uniformity coefficient α for gravel varies down the wall is shown in Figure 1b. The value is again zero at the surface, rising to a stable value of about $\alpha = 2.8$ for most of the wall. It then rises to a peak of $\alpha = 3.7$ before dropping to zero again at the transition. The value derived from the experimental data for the central part of the wall by linear regression was about $\alpha = 3.0$ for gravel.

The least squares best fit tends to give higher values of α than were found in the tests for two reasons. First, the experimental data does not extend across the full width of the wall (pressure cells cannot be located exactly in the corners) and because the deduced value of α is quite sensitive to small changes in the pressure at the centreline. Secondly the best-fit line always tends to under-estimate the pressure at mid-span. The horizontal non-uniformity coefficient α may alternatively be deduced from the "simple" ratio of the two outermost measured data points, giving a relatively accurate representation of the high pressure region. These values are also shown in Figure 1 as the simple ratio.

The comparisons described above show a reasonably close agreement between the experimentally and computationally derived values of α, giving confidence that the same computational analysis may be applied to a wider range of similar problems, and the results exploited in design.

3.1.2 Relative stiffness of the stored granular solid and the silo wall

Both the experimental and computational evidence indicate that the pressure distribution in a square planform silo with flexible walls contains two key features: the mean pressure at any level that is well represented by the Janssen theory, and the distribution of the pressure at each level that is well represented by Eq. 4. The value of the horizontal non-uniformity coefficient α depends on the relative flexibility of the silo walls. The next parts of this study explored the effect of the flexibility of the wall relative to the stiffness of the stored solid.

3.1.3 Stored solid stiffness

For the two stored bulk solids (sand and gravel) used in the tests, many properties are very similar. However the measured lateral pressure distributions were significantly different. The importance of the solid's elastic stiffness to the determination of pressures is now well understood [e.g. 35] and the elastic stiffness of the sand and gravel were significantly different.

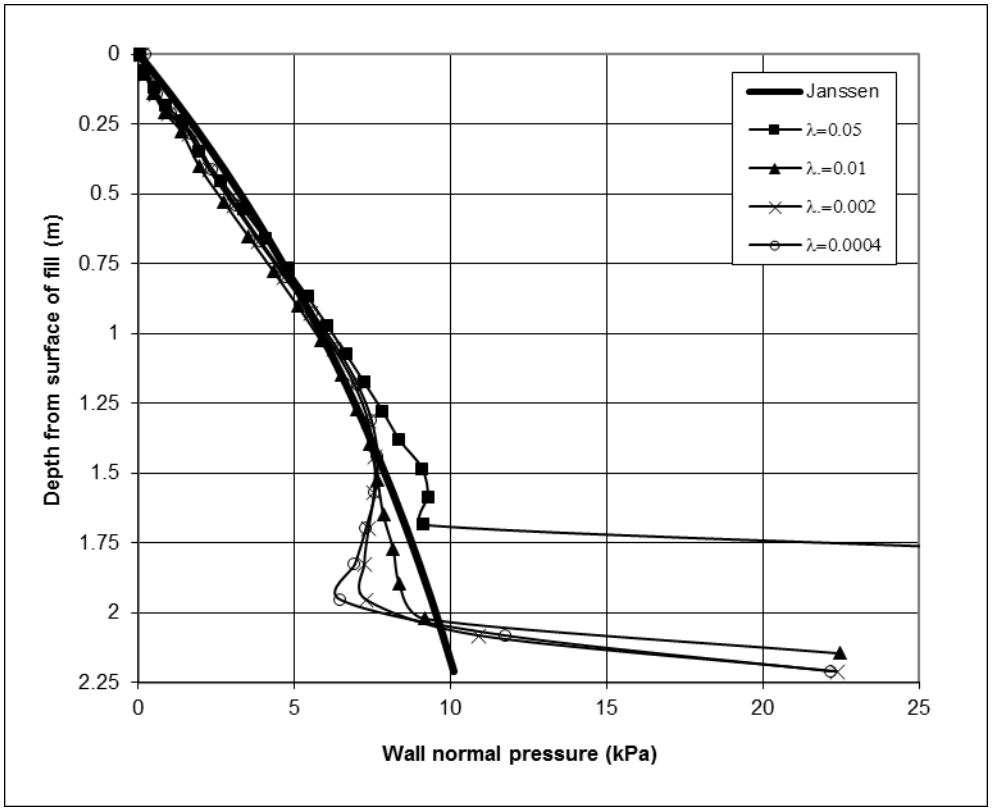

Figure 2 - Wall normal pressure in gravel with variation of compressibility coefficient

In the FE model, the elastic stiffness of the stored solid was characterised by the compressibility coefficient λ (therefore dependent on the stress level) and an initial density (or voids ratio). The mean pressure at each level (mean of the FE calculated pressures on the wall) is affected very little by the value of the compressibility coefficient. Figure 2 shows the lateral pressures computed from the FE model for gravel. The study subsequently uses values of λ of 0.0020 and 0.0025 for sand and gravel respectively. It should be noted that the mean pressures calculated using the Janssen formula (also shown in Figure 2) require the density to be specified, but density varies with stress level. To enable valid comparison, a final density corresponding to the Janssen asymptotic stress level should be

chosen.

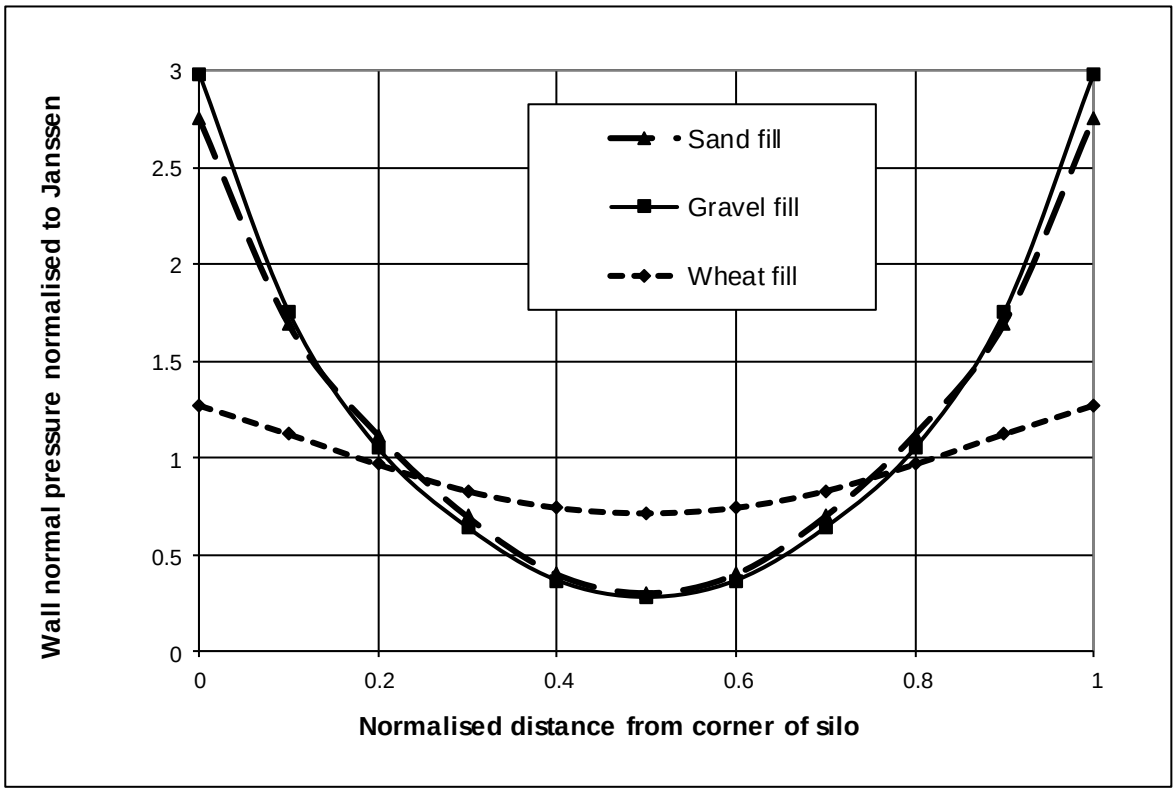

Figure 3 - Patterns of wall pressure from experiment and predicted from FE and empirical models

The distribution of wall pressure at a given level will be different for stored solids whose stiffness characteristics are different from each other. To explore the effects of solid stiffness more completely, wheat was chosen next as a material with very different stiffness characteristics (ν = 0.369, γ=816 kg/m^3, ϕ_i=28˚, μ=0.44, λ=0.021). These values were derived from the tests of Ooi [39] and used in the PEDP model. The results show (Figure 3) that the redistribution of wall pressure is less marked in a softer solid, confirming the view that the distribution is related to the relative stiffnesses of the solid and structure. The determination of the compressibility coefficient at an appropriate pressure level is therefore critically important to the accurate prediction of the distribution of wall pressures in rectangular silos.

3.1.4 Silo wall stiffness

The effect of the relative stiffness of the solid and structure was explored by varying the wall thickness of the silo. Such a change would seem to involve only a single parameter and not demand

careful interpretation, as is needed with changed solids properties. The wall thickness was systematically varied for the modelled silo, with the stored solid taken first as sand and then as gravel. The resulting horizontal pressure distributions at 1.5m below the solid surface are shown in Figure 4. The integrated mean pressure is again always quite close to Janssen value using Eq.1, but the horizontal variation is very sensitive to the wall thickness. When the wall is very stiff (i.e. wall thickness t is large) the wall pressures are close to uniform ($\alpha = 0$). With a very thin wall, a considerable redistribution of pressure from the centre to the corners occurs, but this moves asymptotically towards a second extreme case, which may be characterised as an "ideally flexible" wall.

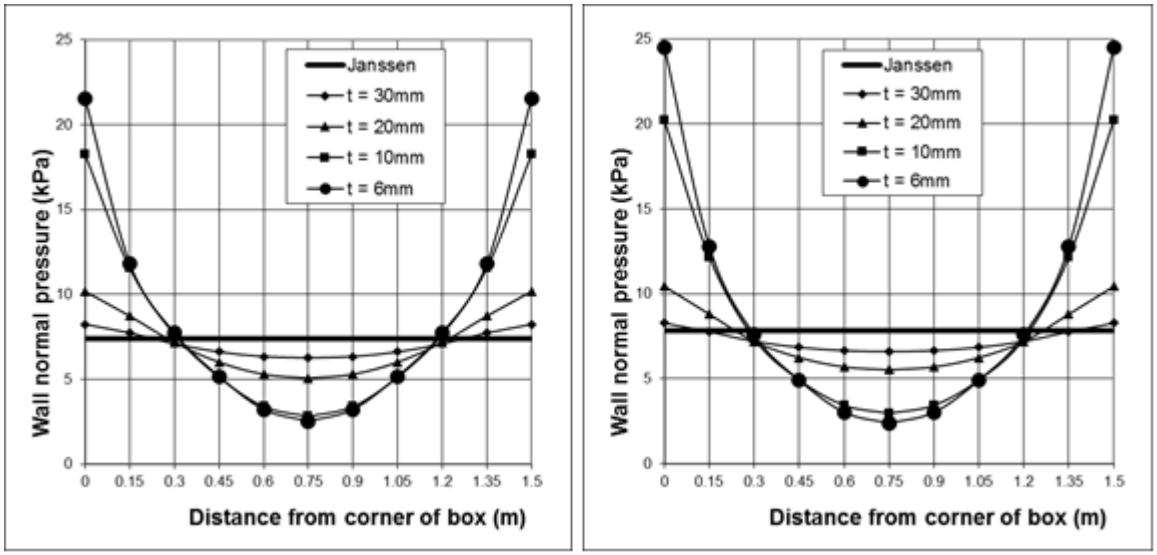

a) b)

Figure 4 - Effect of wall thickness on horizontal pressure distribution. a) sand b) gravel

The effect of varying the modulus of elasticity of the wall alone has been determined for three wall moduli, and the value of α is directly proportional to the variation in E_w (r^2=0.999). Sufficiently large values of modulus are chosen to ensure unreasonable large deflections do not occur with the wall thickness of 6mm used in the study.

3.1.5 Depth within the silo

It has been suggested [11,43] that there should be a reduction in vertical pressure near the corners because elements adjacent to the corner will gain additional frictional support from the two adjacent

walls. There is no evidence of this from the FE results, even for silos with very stiff walls. The dominant mechanism controlling the pressures in rectangular silos is not only wall friction, internal angle and bulk density (the three key parameters used in the Janssen expression), but also the relative stiffness of solid and structure.

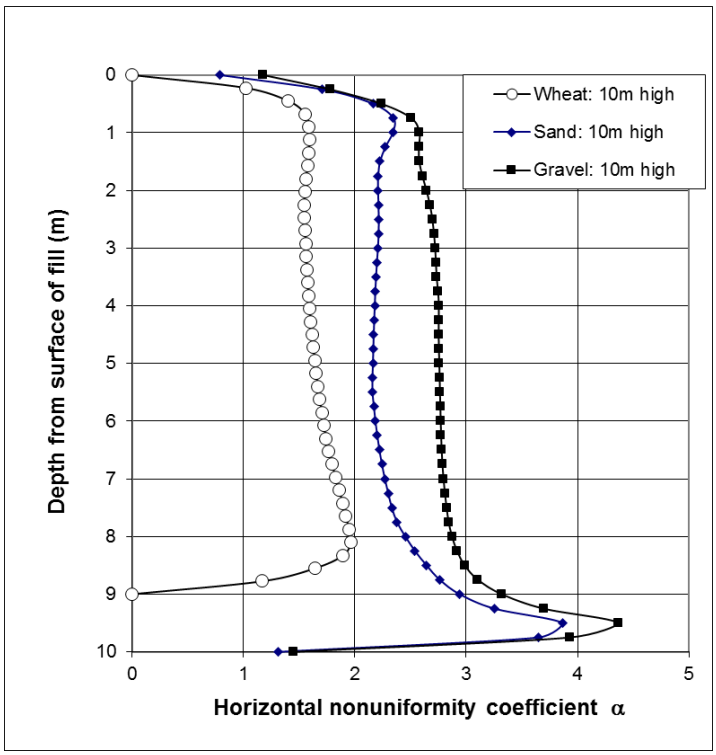

Figure 5 - Variation of α with depth in silo

The extent of pressure redistribution towards the corners varies with the level in the silo. To explore this thoroughly, the pressures in a deep silo (h/L = 6.67) were examined for sand, gravel and wheat (L/t=250). The variation at each level was interpreted in terms of the horizontal non-uniformity coefficient α. The resulting variation of α with depth is shown in Figure 5, where it is evident that the majority of the silo displays a relatively constant value of α for each solid. At the surface, the value approaches zero (uniform pressures), rising to the typical value within a depth of approximately one silo width L. Above the transition, the value rises for sand and gravel before falling to zero, but for the softer wheat, it simply falls. This behaviour is seen over a height of approximately the side length L, though it is less for wheat and greater for sand. The reference value of α, which is fairly stable and

pertains over most of the height, is a useful value by which to characterise the pressure patterns, and this is used in the following design method formulation.

3.1.6 Aspect ratio of silo

The phenomena seen in the deep silo described above also occur in silos of squatter geometries, as shown in Figure 6, where the deduced variation of α for three different silo aspect ratios for the three solids is shown. The transition is at different depths below the surface for the three stored materials. At an intermediate aspect ratio (h/L = 3.33), the two end effects may be seen to occupy the same approximate ranges near the surface and above the transition, with a reduced zone of uniform values in between them. At a squat aspect ratio (h/L = 1.50), the two end effects occupy the whole depth, with the surface and transition effects merging one into the other.

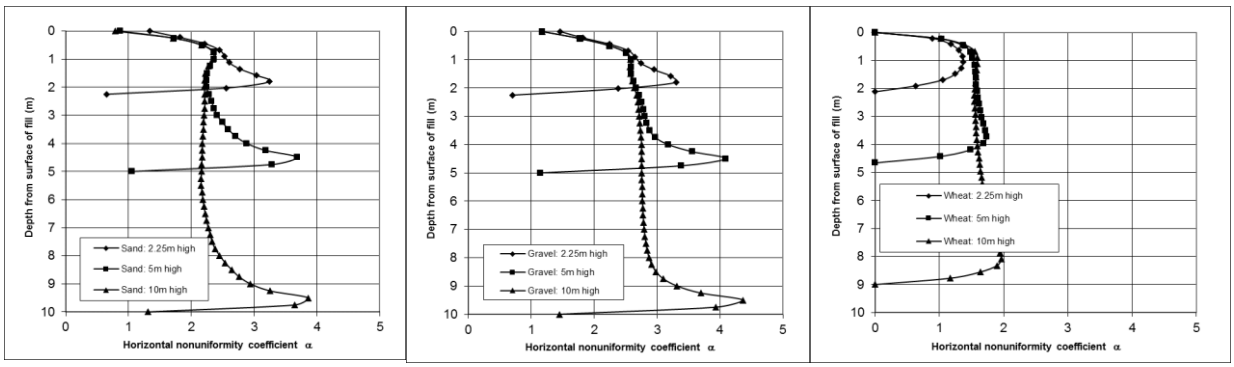

Figure 6 - Variation of alpha for three different materials for different aspect ratios.

The complexity of behaviour seen in the squat silo is not easily transformed into a design rule. However, the value of α is relatively stable over a large part of the height of taller silos, and this value is explored here as a basis for design rule development.

The complete pattern of pressures is thus quite complicated, but the non-uniform pressures in the body of the silo can be safely exploited because the places where α is not at its stable value are parts of the structure that are relatively insensitive to the pressure distribution. Near the surface, the pressures are close to constant (α = 0), but these pressures are so low that the distribution is not critical. Near the transition, both higher and lower values of α occur. A conservative treatment of the structure would adopt a lower value of α, so the high values are not critical. The low value of α at the

transition occurs on a stiff strong structural element (the corner of a box), so this aberration from the general pattern is also not of great concern in a design rule.

4.0 Discussion

4.1 Relative stiffness of solid and silo structure

The calculations described above have shown that the wall pressures are very non-uniform if the stored material is relatively stiff or the wall is relatively flexible. Conversely if the stored material has little stiffness or the wall is very stiff, then the wall pressures are close to uniform, with a low value of α. The stiffness of the wall is dominated by bending deformations, and that of the solid by its elastic stiffness. The relative stiffness is therefore best represented by the dimensionless parameter

$$\rho = \left(\frac{E_S}{E_W}\right)\left(\frac{L}{t}\right)^3 \qquad (5)$$

in which E_W, L, and t are the modulus, side length, and thickness of the silo wall and E_S is the equivalent elastic modulus of the solid. To implement such a relative stiffness, it is necessary to determine the local value of the equivalent linear modulus of the solid E_S that is relevant to the solid-structure interaction. For this purpose, the tangent elastic modulus of the nonlinear porous elastic solid was extracted from the FE analysis using the mean vertical stress at the same level as that at which the value of α has been found.

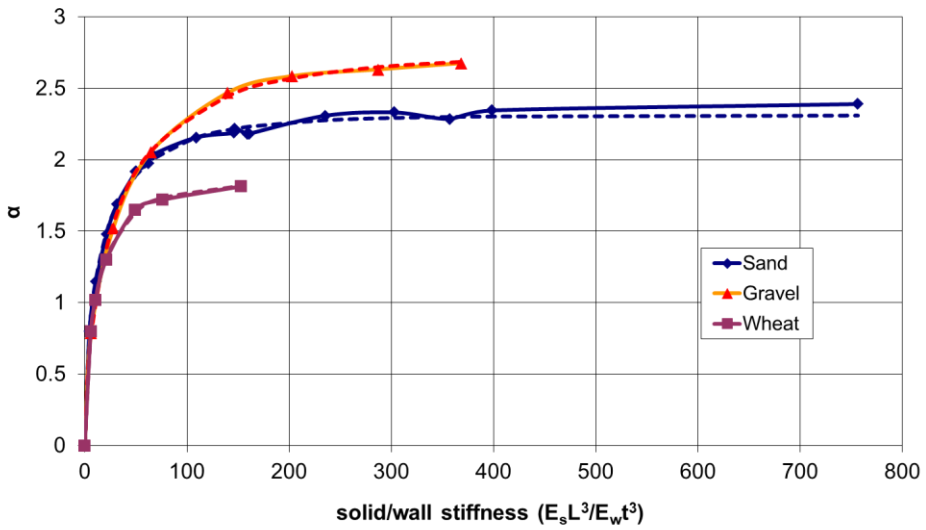

Figure 7 - Variation of α with ρ

The accumulation of results that have been found for a variety of different wall lengths and different wall stiffness is that the variation of the horizontal non-uniformity coefficient α with the relative stiffness ρ can be determined (Figure 7). A relative stiffness of zero corresponds to a very soft solid, for which the pressures remain relatively constant on the entire wall. As the relative stiffness increases, the value of α initially increases rapidly, but it becomes asymptotic to a value of about 2.3 for sand, 2.7 for gravel and 1.8 for wheat. This occurs at relative stiffness values ρ of about 100. These values are close to those found in the experiments by Brown *et al* [8].

When the wall is very thin, large displacements ($\delta > t$) develop in the wall, resulting in a change in geometry, and the simple picture of Figure 7 is lost as α rises further. Calculations involving large displacements of the wall have therefore been omitted. This situation arose with wheat when the value of ρ was about 150.

These results are not usable in design until they can be represented in a dimensionless manner. Therefore, the prediction of this behaviour deserves further study, as significant savings might be made if lower mid-side pressures can be used in design. This prediction can be made from the dataset described above, assuming an exponential form and using a goal-seek algorithm in Microsoft Excel to obtain the best fit for the unknown coefficients. A remarkably good fit to the relationships for the materials shown is found as:

$$\alpha = \alpha_o \{ 1 - e^{-[(\rho/(4\alpha_o^2)]^{0.6}} \} \qquad (6)$$

which is shown by the dotted lines in Figure 7. However it may be that other material parameters weakly affect this relationship. The value of α_o depends on the properties of the granular solid, and future investigations are needed to produce relations for α that have application to a wider range of granular solids, but based on the above data it can be closely represented (r^2=1.0) by

$$\alpha_o = \frac{0.47}{K_o \mu} \qquad (7)$$

in which $K_o = \nu / (1 + \nu)$ (see also Eq. 1). (Figure 8)

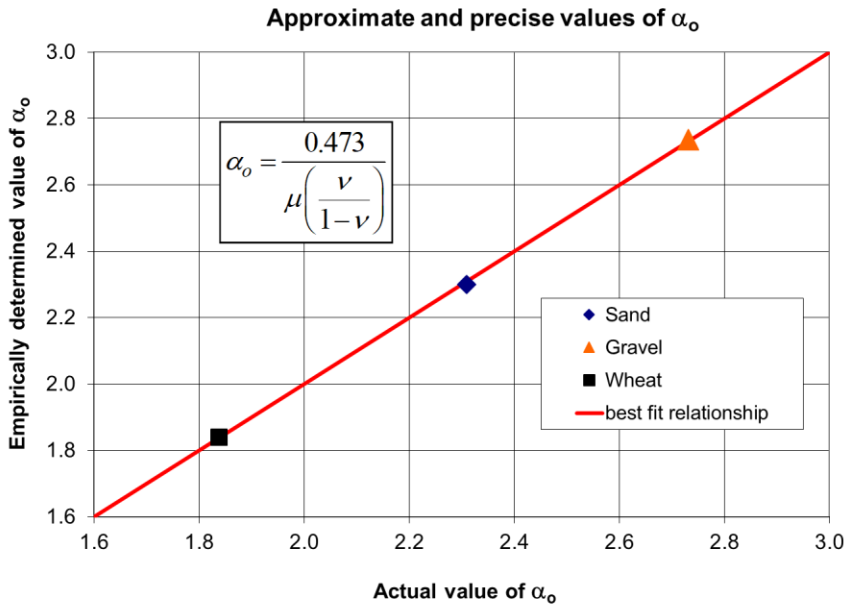

Figure 8 - Correlation of α_0

It should be noted that, although the above correlation is very close and uses plausible parameters, it is empirically based on relatively limited data. However, it may serve as a useful guide in future investigations that attempt to produce relations for α that have application to a wider range of granular solids.

5.0 Conclusions

A non-linear elastic-plastic constitutive 3D finite element model has been used to predict the pressures in square planform thin-walled silos filled with three different solids. The calculations have been strongly supported by a remarkably close correlation with the experimental results on test silos. The chosen constitutive model involved a limited number of parameters to maximise the potential for the results to be applied in design, where limited information is available concerning material properties.

The mean wall pressure at any level is close to the Janssen prediction, but the horizontal distribution is far from uniform and is sensitive to the flexibility of the wall. In thin-walled silos, high pressures develop in the corners, with corresponding low pressures at the mid-side. If this effect can be exploited in design, the wall can be made much thinner, leading to greater wall flexibility, which in turn leads to a greater redistribution of pressures into the corners.

The simple two-parameter empirical model proposed by Rotter *et al* [21] gives a very good description of the horizontal pressure distribution at all levels for both the experimental data and calculations, characterised by the horizontal non-uniformity coefficient α. These subsequent calculations presented above have shown that the extent of redistribution depends on the relative stiffness of the solid and wall, characterised by the parameter ρ. At low ρ, the pressures on the wall are uniform, but where ρ exceeds about 100, the amount of redistribution remains unchanging at a value that depends on the stored solid.

A simple preliminary empirical relationship has been developed to predict the value of the horizontal non-uniformity coefficient α as a function of the stiffness ratio ρ, but a further study is required to extend this relationship to design rules. However, provided the relevant solid stiffness E_S can be evaluated satisfactorily, a relationship of this type could be adopted into design procedures to achieve efficient structural designs for square planform silos.

References

1. Gaylord, E.H. and Gaylord, C.N., Design of Steel Bins for Storage of Bulk Solids, Prentice Hall. 1984
2. Brown, C.J., “Rectangular Silo Structures” in Silos; Fundamentals of Theory Behaviour and Design (Brown C.J. and Nielsen J. eds) Spon, 1998, 426-442
3. EN1993-4-1, - Design of steel structures - Part 4-1: Silos, 2007
4. Trahair, N.S., Abel, A., Ansourian, P., Irvine, H.M., and Rotter, J.M., Structural Design of Steel Bins for Bulk Solids, Australian Institution of Steel Construction, Sydney, 1983
5. Rotter, J.M., "Membrane Theory of Shells for Bins and Silos", Transactions of Mechanical Engineering, Institution of Engineers, Australia, Vol. ME12 No.3 September 1987, 135-147.
6. Rotter, J.M. "Bending Theory of Shells for Bins and Silos", Transactions of Mechanical Engineering, Institution of Engineers, Australia, Vol. ME12 No.3 September 1987, pp 147-159.
7. Rotter, J.M. Guide for the economic design of circular metal silos. Spon Press, London, 2001
8. Brown, C.J., Lahlouh, E.H. and Rotter, J.M., “Experiments on a Square Planform Silo”, Chem. Eng. Sci., 2000, Vol 55, No 20, 4399-4413
9. Janssen, H.A. “Versuche über getreidedruck in silozellen”, Zeitshrift des Vereines Deutscher Ingenieure, 39 (35), 1045-1049. 1895.
10. Reimbert, M. and Reimbert, A., Silos: Theory and Practice, Trans Tech Publications, 1976.
11. Ragneau E., Aribert J.M., and Sanad A.M. “Modèle tri-dimensionnel aux éléments finis pour le calcul des actions sur les parois d'un silo (remplissage et vidange)”, Construction Metallique, 1994, 2, 3-25.
12. Jarrett, N.D., Brown, C.J., and Moore, D.B. “Pressure measurements in a rectangular silo”, Geotechnique, 1994, 44 (3), 95-104.
13. Lahlouh, E.H., Brown, C.J., and Rotter, J.M. “Loads on rectangular planform steel silos”, Res. Rep. No. 95-027, Univ. of Edinburgh, U.K., 1995

14. Häussler, U. and Eibl, J., "Numerical investigations on discharging silos", Jnl. Eng. Mech. Divn., ASCE, 1984, 110, 957-971

15. Gudehus, G., Kolymbas, D. and Tejchman, J., "Behaviour of granular materials in cylindrical silos", Powder Technology, 1986, 48, 81-90

16. Link, R.A. and Elwi, A.E., "Incipient flow in silo-hopper configurations", Jnl. Eng. Mech. Divn., ASCE, 1990, 116(1), 172-188

17. Ruckenbrod, C., and Eibl, J. "Numerical results to discharge processes in silos", Int. Symp.: Reliable Flow of Particulate Solids II, Proc. EFChE Publication Series No. 96, Oslo, Norway, August 1993, 503-516

18. Ragneau, E., Ooi, J.Y. and Rotter, J.M., "Finite element models for specific applications" in Silos; Fundamentals of Theory Behaviour and Design (Brown C.J. and Nielsen J. eds) Spon, 1998, 495-508

19. Gallego, E., Goodey, R., Ayuga, F,. and Brown, C.J., "Some Practical Features in Modelling Silos with Finite Elements". Paper number 044150, 2004 ASAE Annual Meeting (doi: 10.13031/2013.16825) 2004

20. Rotter, J.M., Holst, J.M.F.G, Ooi, J.Y. and Sanad, A.M., "Silo pressure predictions using discrete-element and finite-element analyses", Phil. Trans. R. Soc. London, 1998, 356, 2685-2712

21. Rotter, J.M., Brown, C.J., and Lahlouh, E.H., "Patterns Of Wall Pressure on Filling a Square Planform Steel Silo" Engineering Structures, Vol. 24, pp.135-150, 2002

22. Bishara, A.G., Mahmoud, M.H. and Chandrangsu, K. "Finite Element Formulation for Farm Silo Analysis", Journal of the Structural Division, ASCE, Vol. 103, No. 10, October, pp 1903-1919. 1977

23. Ding, S., Rotter, J.M., Ooi, J.Y. and Enstad, G. "Development of normal pressure and frictional traction along the walls of a steep conical hopper during filling", Thin-Walled Structures, Vol. 49, No. 10, Oct. 2011, pp 1246-1250.

24. Meng, Q., Jofriet, J.C. and Negi, S.C. “Finite Element Analysis of Bulk Solids Flow: Part 1, Development of a Model Based on a Secant Constitutive Relationship”, J. Agricultural Engineering Research, Vol. 67, No. 2, June, pp. 141-150. 1997

25. Karlsson, P., Klisinski, M. and Runesson, K. “Finite element simulation of granular material flow in plane silos with complicated geometry”, Powder Technology, Vol. 99, Issue 1, 1 September, pp. 29-39, 1998

26. Vidal, P., Couto, A., Ayuga, F. and Guaita, M. Influence of hopper eccentricity on discharge of cylindrical mass flow silos with rigid walls. Journal of Engineering Mechanics, ASCE, 132 (9) 1026 - 1033. 2006

27. Ding, S., Li, H., Ooi, J.Y., and Rotter, J.M., “Prediction of flow patterns during silo discharges using a finite element approach and its preliminary experimental verification”, Particuology, Vol 18, 2015, 42-49

28. DS Simulia. "Abaqus/CAE user's manual". 2010.

29. Goodey, R.J., Brown, C.J. and Rotter, J.M. “Verification of a 3-dimensional model for filling pressures in square thin-walled silos”, Engineering Structures, Vol. 25, No. 14, pp. 1773-1783. 2003

30. Goodey, R.J., Brown, C.J. and Rotter, J.M. “Verification of a 3-dimensional model for filling pressures in square thin-walled silos”, Engineering Structures, Vol. 25, No. 14, pp. 1773-1783. 2006

31. Goodey, R.J., Brown, C.J. and Rotter, J.M. “Rectangular steel silos: Finite element predictions of filling wall pressures”, Engineering Structures 132 (2017) pp. 61–69 2017

32. Ooi, J.Y., Chen, J.F., Lohnes, R.A. and Rotter, J.M., “Prediction of static wall pressures in coal silos”, Construction and Building Materials, 1996, 10 (2), 109-116

33. Ooi J.Y. and She K.M. “Finite element analysis of wall pressure in imperfect silos”, Int. J. Solids Struct, 34(16), pp. 2061–72. 1997

34. Ding, S. and Enstad, G. G. “FE approach to the sensitivity of load on a hopper to the filling method and process with granular material”, Proceedings of IMECE’03 ASME International

Mechanical Engineering Congress & Exposition, Washington, D.C., USA, November 16-21. 2003

35. Muir Wood, D. “Soil behaviour and critical state soil mechanics”, Cambridge University Press, Cambridge, England, 1990
36. EN1991-4 Eurocode 1: Basis of design and actions on structures, Part 4 – Silos and tanks, Eurocode 1 Part 4, CEN, Brussels, 2006
37. Ooi, J.Y. and Rotter J.M., “Wall pressures in squat steel silos from simple finite element analysis”, Computers and Structures, 1990, 37 (4), 361-374
38. Garnier J., Ternet, O., Cottineau. L-M., and Brown C.J., “Placement of embedded pressure cells” Geotechnique, Volume 49, Issue 3, June 1999, pp. 415-421
39. Ooi, J.Y. Bulk Solids Behaviour and Silo Wall Pressures, PhD Thesis, School of Civil and Mining Engineering, University of Sydney, Australia, 1990
40. Been, K., Jefferies, M.G. and Hachey, J., “The critical state of sands”, Géotechnique, 1991, 41 (3), 365-381
41. Goodey, R.J. and Brown, C.J. “The influence of the base boundary condition in modelling a metal silo”, Computers and Structures, Vol. 82, pp. 567-579. 2004
42. Jarrett, N.D., Brown, C.J. and Moore, D.B. "Stress Redistribution in Rectangular Planform Silos", Geotechnique, vol. 45, no. 1, pp. 95-104. 1995
43. AS 3774-1990 “Loads on Bulk Solids Containers”, Australian Standard with Commentary, Standards Association of Australia, Sydney, 1990.

Acknowledgement

This research did not receive any specific grant from funding agencies in the public, commercial, or not-for-profit sectors.

APPENDIX

	Mean Angle of internal friction from Table E1 [3]	Mean Lateral pressure ratio K from Table E1 [3]	Poisson's ratio calculated from Eq. 2	Poisson's ratio calculated from Eq. 3	percentage error
Default material	35	0.5	0.3333	0.3191	-4.3
Aggregate	31	0.52	0.3421	0.3477	1.6
Alumina	30	0.54	0.3506	0.3546	1.1
Animal feed mix	36	0.45	0.3103	0.3118	0.5
Animal feed pellets	35	0.47	0.3197	0.3191	-0.2
Barley	28	0.59	0.3711	0.3683	-0.7
Cement	30	0.54	0.3506	0.3546	1.1
Cement clinker	40	0.38	0.2754	0.2819	2.4
Coal	31	0.52	0.3421	0.3477	1.6
Coal powdered	27	0.58	0.3671	0.3750	2.2
Coke	31	0.52	0.3421	0.3477	1.6
Fly ash	35	0.46	0.3151	0.3191	1.3
Flour	42	0.36	0.2647	0.2666	0.7
Iron ore pellets	31	0.52	0.3421	0.3477	1.6
Lime hydrated	27	0.58	0.3671	0.3750	2.2
Limestone powder	30	0.54	0.3506	0.3546	1.1
Maize	31	0.53	0.3464	0.3477	0.4
Phosphate	29	0.56	0.3590	0.3615	0.7
Potatoes	30	0.54	0.3506	0.3546	1.1
Sand	36	0.45	0.3103	0.3118	0.5
Slag clinkers	36	0.45	0.3103	0.3118	0.5
Soya beans	25	0.63	0.3865	0.3882	0.4
Sugar	32	0.5	0.3333	0.3406	2.2
Sugar beet pellets	31	0.52	0.3421	0.3477	1.6
Wheat	30	0.54	0.3506	0.3546	1.1

Appendix - Typical values for Poisson's ratio